Soft Matter

PAPER

View Article Online
View Journal | View Issue

Cite this: *Soft Matter*, 2017, 13, 2004

Unusual nanosized associates of carboxy-calix[4]resorcinarene and cetylpyridinium chloride: the macrocycle as a glue for surfactant micelles†

Ju. E. Morozova,*[ab] V. V. Syakaev,[a] Ya. V. Shalaeva,[ab] A. M. Ermakova,[ab] I. R. Nizameev,[ac] M. K. Kadirov,[a] A. D. Voloshina,[a] V. V. Zobov,[a] I. S. Antipin[ab] and A. I. Konovalov[a]

Received 2nd January 2017,
Accepted 24th January 2017

DOI: 10.1039/c7sm00004a

rsc.li/soft-matter-journal

The association of cetylpyridinium chloride (CPC) micelles in the presence of octaacetated tetraphenylene-oxymethylcalix[4]resorcinarene (CR) leads to the formation of unusual spherical supramolecular nanoparticles (SNPs). Within the range of CR/CPC molar ratios from 10/1 to 1/10 (except for 1/8), CR, acting as a counterion, decreases the critical micelle concentration of CPC by one order of magnitude and leads to the formation of SNPs with an average hydrodynamic radius of 164 nm and an average zeta potential of −60 mV. The formation of SNPs was studied by NMR FT-PGSE and 2D NOESY, DLS, TEM, fluorimetry, and UV-Vis methods. The stability of SNPs at different temperatures and pH values and in the presence of electrolytes was investigated. The specificity of the interactions of the SNPs with substrates that were preferentially bound by a macrocycle or CPC micelle was studied. The enhancement of cation dye binding in the presence of SNPs is shown. The presented supramolecular system may serve as a nanocapsule for water-soluble and water-insoluble compounds.

Introduction

The design of nanosized supramolecular assemblies presents an opportunity to construct multifunctional smart materials and nanocontainers.[1] The advantages of the supramolecular approach to their creation are reproducible non-covalent synthesis, which allows precise control of the composition and morphology of the systems from batch-to-batch, and non-covalent substrate encapsulation with a high loading efficiency.[2] Spontaneously organized self-associates in solutions of different amphiphilic compounds (polymers,[3] macrocycles,[4] and surfactants[5]) and their co-associates (polymer–polymer,[6] polymer–surfactant,[7] polymer–macrocycles,[1a,b] oppositely charged surfactants,[8] and surfactant–macrocycles[1a,b]) belong to these systems. In polymeric nanosystems, hydrophilic polymers non-covalently bind the molecules and micelles of surfactants. Usually, the size of these nanosystems depends on the size of the polymer molecules.[9] The interaction of the oppositely charged surfactants leads to the formation of cationic amphiphiles that spontaneously form vesicles.[8] When co-association occurs between the macrocycles and the surfactants, the obtained supramolecular systems may have a different morphology, such as bilayers or micellar structures.[10]

Recently, calixarenes and calixresorcinarenes have been intensively used as components of supramolecular assemblies.[11] This is due to their ability to form host–guest complexes through various non-covalent interactions (π–π, CH–π, cation–π, electrostatic, H-bonding, and hydrophobic, depending on the functionalization of the macrocycles) and their ability to be functionalized by different groups on the upper and lower rims and to adopt different conformations. Together with their low toxicity,[12] these features lead to the potential applications of calixarenes and calixresorcinarenes as components of drug delivery systems because these nanostructures are easily tuned and also respond to several external stimuli, such as temperature, pH, voltage, redox, and light.[1b]

Calixarenes bearing charged groups can easily interact with oppositely charged surfactants to form nanosized supramolecular systems. The macrocycle and the surfactant can form a host–guest complex[13] or ion pair[14] in the solution. Commonly, the co-association of a surfactant with amphiphilic calixarenes,

[a] *A. E. Arbuzov Institute of Organic and Physical Chemistry, Kazan Scientific Center, Russian Academy of Science, Arbuzov str. 8, 420088 Kazan, Russian Federation. E-mail: moroz@iopc.ru*
[b] *Kazan Federal University, Kremlevskaya st. 18, 420008 Kazan, Russian Federation*
[c] *Kazan National Research Technical University, K. Marx str. 10, 420111 Kazan, Russian Federation*

† Electronic supplementary information (ESI) available: Tables S1–S7, and Fig. S1–S8. The details of the study of fluorescence anisotropy of DPH in CR–CPC solutions, the cca-values study of CR–CPC (1/1) and CPC in 0.15 M NaCl and PB (pH 7.4), and study of the complex stability constant of R6G with CR and SNPs. See DOI: 10.1039/c7sm00004a

whose molecules contain long alkyl substituents and are capable of self-association, leads to the formation of cationic amphiphiles that spontaneously associate into vesicular structures.[15] Another example is hydrophilic calixarenes that exist as monomers or form non-classic head-to-tail associates in aqueous solution. These macrocycles can create both micellar[13b,16] and vesicular assemblies[13a,17] with oppositely charged surfactants.

The results of the investigation of surfactant–calixarenes/calixresorcinarenes showed that the addition of macrocycles usually decreases the cmc of the surfactant.[13,15,16a,17a,18] Herewith, the solubilization capability of the surfactant micelles toward hydrophobic compounds is decreased as a result of the reassembly of surfactant micelles and disruption of the hydrophobic core.[19] Nevertheless, such systems are probably able to bind hydrophilic compounds that are complementary to the macrocycle. It is known that the inclusion of water-soluble drugs into nanocapsules protects them from biodegradation and promotes both slow release and the possibility of controlling their entry using external stimuli (pH, temperature, and the addition of concurrent guest molecules).[20] There are no experimental facts on changes in the binding capacity resulting from the incorporation of macrocycles in co-associates with surfactants. It is known that in comparison with macrocyclic monomers, the binding of guest molecules by calixresorcinarene self-associates is increased due to the cooperative action of macrocyclic molecules.[21] Therefore, the binding capacity of macrocycles in surfactant–calixresorcinarene systems can be advantageous with respect to the formation of nanocontainers. The aim of our study is the design of a novel supramolecular surfactant–calixresorcinarene system, cetylpyridinium chloride (CPC)–octaacetated tetraphenyleneoxymethylcalix[4]resorcinarene (CR), the investigation of its structure and morphology, and the estimation of its binding to some substrates.

CPC has been chosen as a cationic surfactant because of its structural features, micellar properties, and sphere of application. CPC has a pyridinium group, which is a highly complementary guest fragment for anionic calixarene and calixresorcinarene due to its ability to take part in cation–π interactions.[22] CPC is used in drug formulations[23] and as an antibacterial agent.[24] It is known that the presence of organic compounds (long-chain alcohols,[25] hydrotropes[26]) and bulky inorganic anions[27] (Br^-, NO_3^-, ClO_3) leads to microstructural micelle – rod-like micelle changes in CPC solutions, accompanied by an increase in their viscosity.[28] The cmc of CPC is about 0.9–1 mM.[26] The addition of hydrotropes (salicylate, benzoate anions) decreases the cmc by one or two orders of magnitude depending on their concentration; at the same time, solutions begin to develop viscoelastic properties due to the formation of rod-like micelles.[26]

The participation of CPC in the formation of supramolecular systems with cucurbit[*n*]urils (CB, n = 5, 7) has been studied.[29] The formation of the ion pair CB5–CPC leads to a decrease in the CPC cmc (from 1 to 0.57 mM), and the formation of an inclusion complex with the larger CB7 leads to an increase in the cmc (to 1.63 mM). The serial addition of CB5 or CB7 to the CPC solution or increasing of the temperature allows control of the cmc, which leads to controlled release of a dye (Nile red) from the micelle and allows such systems to be used as a supramolecular smart drug delivery device.[29]

Here, we have studied the formation of a supramolecular system of CPC with octacarboxylic calixresorcinarene bearing four methoxyphenylene groups on the lower rim of CR (Fig. 1). It has previously been shown that CR does not form self-associates in aqueous solution but forms a host–guest complex with cationic dye crystal violet (CV) with 46% of bound guest (FT-PGSE NMR).[21c] At the same time, analogs of CR bearing long aliphatic substituents on the lower rim (pentyl, pentyloxyphenylene, octyl, undecyl, dodecyloxyphenylene) include CV in macrocyclic self-associates between macrocyclic molecules, which leads to almost 100% guest binding even where there is an excess of guest in the solution.[21c] Therefore, it was necessary to investigate the effect of CR on the guest binding under the conditions of its forced inclusion into a co-association with a surfactant. Thus, the aim of the present investigation was to study the characteristics of interactions in the CPC–CR supramolecular system, to determine the influence of CR on the morphology of CPC micellization, and to study the change in the binding properties of the CPC–CR system towards guests, which are complementary to those of CPC micelles and CR.

Experimental

Calixresorcinarene (CR) was synthesized according to a previously reported procedure.[21c] Cetylpyridinium chloride (Sigma-Aldrich, India), pyrene (Sigma-Aldrich, Switzerland), methyl yellow (Sigma-Aldrich, Russia), and rhodamine 6G (Acros, USA) were used as received. Pentylpyridinium bromide was synthesized from pyridine and 1-bromopentane in dry MeOH under reflux and characterized by ^{1}H NMR spectroscopy (see ESI†).

NMR spectroscopy

All NMR experiments were performed on a Bruker AVANCE-500 spectrometer. The spectrometer was equipped with a Bruker multinuclear z-gradient inverse probe head capable of producing gradients with a strength of 50 G cm^{-1}. All experiments were carried out at 303 ± 0.2 K. Chemical shifts (δ) were reported relative to HDO (4.700 ppm) as an internal standard. Fourier transform pulsed-gradient spin-echo (FT-PGSE) experiments were performed using the BPP-STE-LED (bipolar pulse pair-stimulated echo-longitudinal eddy current delay) sequence. Data were acquired with a 50.0 ms diffusion delay with a bipolar gradient pulse duration from 3.0 to 4.8 ms (depending on the system under investigation), a 1.1 ms spoil gradient pulse (30%), and a 5.0 ms eddy current delay. The bipolar pulse gradient strength was varied incrementally from 0.01 to 0.32 T m^{-1} in 16 steps. The temperature was set and controlled at 303 K with a 600 l h^{-1} air flow rate in order to minimize convection effects. The diffusion experiments were performed at least three times and only the data with correlation coefficients of a natural logarithm of the normalized signal attenuation ($\ln I/I_0$) as a function of the gradient amplitude $b = \gamma^2\delta^2g^2(\Delta - \delta/3)$ (γ is the gyromagnetic ratio, g is the pulsed gradient strength, Δ is the

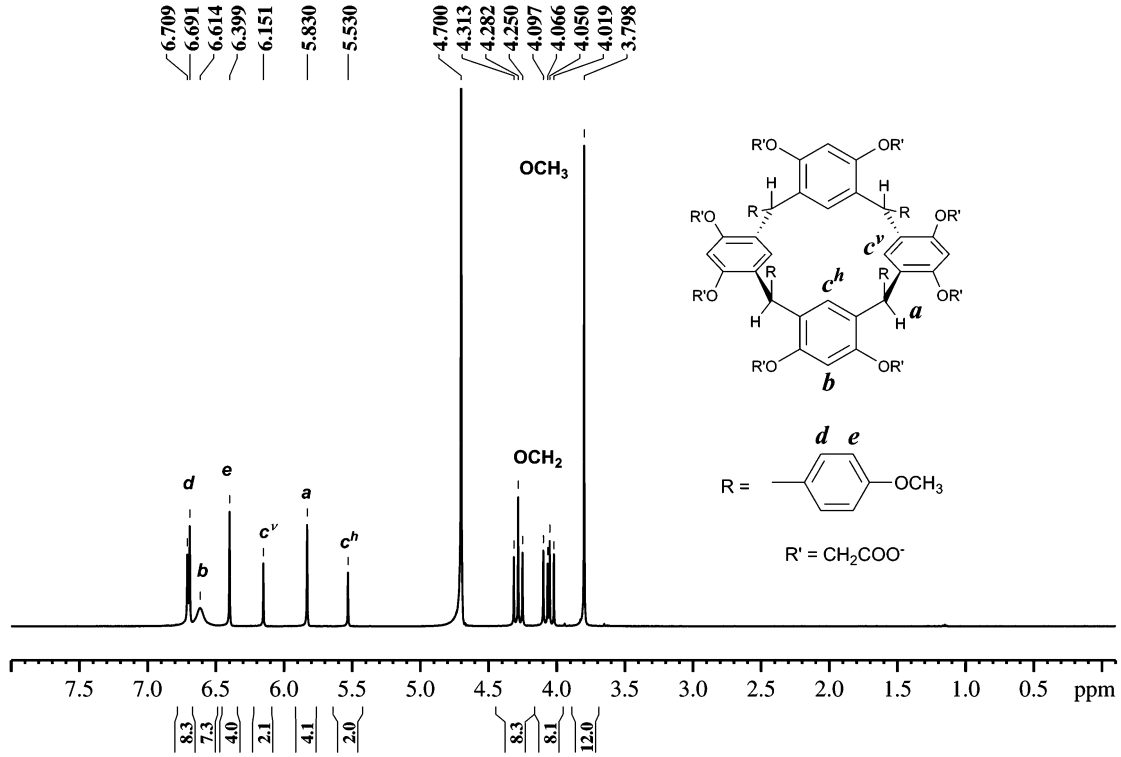

Fig. 1 The structure of CR and its ^{1}H NMR spectrum in D_2O (500 MHz).

time separation between the pulsed-gradients, and δ is the duration of the pulse) that were higher than 0.999 were included.

After Fourier transformation and baseline correction, the diffusion dimension was processed with the ''T1/T2 Analysis Module'' of the Bruker XwinNMR software package (version 3.5). The diffusion constants were calculated by exponential fitting of the data belonging to individual columns of the pseudo 2D matrix. Single components have been assumed for the fitting routine. All separated peaks were analyzed and the average values were presented.

The aggregation number N_{ag} was calculated as: $N_{ag} = (R_H^{exp}/R_H^{teor})^3$, where R_H^{exp} and R_H^{teor} are the experimental and theoretical hydrodynamic radii of the molecules. The values of R_H^{teor} of CR (which complies with the R_H of the monomer) were estimated with the help of the HYDRONMR program.[30]

The 2D NOESY experiments were performed with mixing times of 50–400 ms with pulsed filtered gradient techniques. The pulse programs for all NMR experiments were taken from the Bruker software library.

Dynamic light scattering and zeta potential measurements

Dynamic light scattering (DLS) measurements were carried out on a Zetasizer nano ZS (Malvern Instruments Ltd, England) using Dispersion Technology Software 5.00. The measurements were carried out at room temperature in polystyrol cells; for temperature-dependent measurements, (25–60 °C) a glass cuvette (PCS8501, Malvern) was used. Each CR–CPC combination (ESI,† Table S1) was tested in at least three identical solutions. The error of the hydrodynamic particle size determination was $<2\%$.

A Zeta-potential Nano-ZS instrument (MALVERN) with laser Doppler velocimetry and phase analysis light scattering was used for zeta potential measurements. The measurements were carried out in folded capillary cells (DTS1061, Malvern). The temperature of the scattering cell was controlled at 25 °C; the data were analyzed with the software supplied for the instrument.

TEM measurements

The transmission electron microscopy (TEM) images were obtained with a Hitachi HT7700 instrument, Japan. The images were acquired at an accelerating voltage of 100 kV. Samples were dispersed on 300 mesh copper grids with continuous carbon-Formvar support films.

Fluorescence measurements

Fluorescence emission spectra were obtained on a Varian Cary Eclipse fluorescence spectrophotometer (USA). A quartz cell of 1 cm path length was used for all fluorescence measurements.

The critical micelle concentration (cmc) in deionized water and in the presence of NaCl, and the critical association concentration (cac) of CPC in the presence of CR, were determined using fluorescence spectra of pyrene (0.002 mM). Pyrene was excited at 333 nm, the emission spectra were recorded from 345–500 nm, and the excitation and emission slit widths were 5 nm. The ratio of the first (372 nm) to the third (381 nm) emission band, I/III, for every spectrum was estimated and the cac values were determined from the dependence of I/III on the macrocycle concentration.[31]

Rhodamine 6G (R6G, 0.038 mM) was excited at 500 nm, emission spectra were recorded from 520–700 nm, and the fluorescence intensity was measured at 562 nm. The excitation and emission slit widths were 2.5 and 1.5 nm, respectively. The absorbance and fluorescence spectra of R6G were recorded in the absence and presence of CR (0.909 mM), CPC (0.909 mM), and CPC/CR 1/1 (0.909 mM).

Solubilization of methyl yellow

The solubilization experiments were performed by adding an excess of the crystalline dye methyl yellow (MY) to aqueous solutions of CR (2.86 mM), CPC (1 mM), CR–CPC 4/1 (C(CPC) = 0.976 mM, C(CR) = 0.244 mM), and CPC/CR 1/4 (C(CPC) = 0.714 mM, C(CR) = 2.86 mM) mixtures. The solutions were mixed at 20 °C for 4 h at a rate of 360 rpm. They were then centrifuged (rate 6 krpm, 10 min, centrifuge Eva-20 (Hettich Zentrifugen, Germany)) to separate non-solubilized MY. The UV Vis spectra of the obtained solutions were registered on a Lambda 35 UV-Vis Spectrometer (Perkin-Elmer Instruments, USA) using quartz cells with an optical path of 0.1 cm.

The study of stoichiometry of CPC/CR by UV/Vis method

A number of CPC/CR solutions with constant concentrations of CPC (0.1 and 0.5 mM) and different CR/CPC molar ratios (from 10/1 to 1/8) were prepared. The absorbance at 500 nm was measured with a Lambda 35 UV-Vis spectrometer (Perkin-Elmer Instruments, USA) using quartz cells with an optical path of 0.2 cm.

Hemolysis of human red blood cells

The CR was tested for its hemolytic activity against human red blood cells (hRBC). Fresh hRBC with heparin was rinsed 3 times by centrifugation with 0.15 M NaCl for 10 min at 800g and resuspended in 0.15 M NaCl. CR was dissolved in 0.15 M NaCl and added to 0.5 mL of a solution of the stock hRBC in 0.15 M NaCl to reach a final volume of 5 mL (final erythrocyte concentration, 10% v/v). The resulting suspension was incubated under agitation for 1 h at 37 °C. The sample was centrifuged at 2000g for 10 min. The release of hemoglobin was monitored by measuring the absorbance of the supernatant at 540 nm. The controls for zero hemolysis (blank) and 100% hemolysis consisted of hRBC suspended in 0.15 M NaCl and distilled water, respectively.

Results and discussion

The data for CR individual solutions

Macrocycle CR is soluble in aqueous solution and practically insoluble in organic solvents due to eight anionic groups on the upper rim. In the ^{1}H NMR spectrum of CR in D_2O solution, doubling of signals of ArH^c protons and the high symmetry of location of these signals and signal of methine bridge protons c^v-a-c^h (Fig. 1) are observed, which indicate the existence of CR molecules in a chair conformation.[32] According to NMR FT-PGSE data, an increase in the CR concentration practically has no influence on its self-diffusion coefficient, D_s (Table 1). The values of the average aggregation number N_{ag} are about 2.2–2.3, which apparently indicates the presence of a tight and stable solvate shell around the CR molecules.[21c]

To study the potential use of CR in drug delivery systems, its toxicity to human red blood cells was studied. The experiment showed that 0% erythrocyte hemolysis was observed in the presence of 0.5 mM CR (Fig. S1, ESI†). The low toxicity of CR can probably be explained by the presence of anionic groups and by the absence of long aliphatic substituents in the macrocyclic molecule.

The study of CR–CPC solutions at different molar ratios of components

The addition of amphiphilic calixresorcinarenes to solutions of oppositely charged surfactants usually leads to the inclusion of macrocyclic molecules into the surfactant micelles and to a decrease in their cmc values due to the increase in the hydrophobicity of the mixed associate.[13b,15,16a,17a,18b,33] The concentration range over which the mixed associates exist depends on the molar macrocycle/surfactant ratio, and an excess of one component leads to an increase in the amount of surfactant or amphiphilic calixresorcinarene self-associates.[15,33]

Initially, CPC–CR solutions with CPC/CR molar ratios from 30/1 to 1/20 were prepared (the concentration of CPC was varied from 0.5 mM to 1 mM, Table S1, ESI†). All solutions with CPC/CR

Table 1 The NMR FT-PGSE data for CR, CPC, and CR–CPC solutions in D_2O: D_s – self-diffusion coefficient, R_H^{exp} – experimental hydrodynamic radii of CR, N_{ag} – the average aggregation number

	C, mM			CR			CPC	
	CR	CPC	C(CPC)/C(CR)	$D_s \times 10^{-10}$, m^2 s^{-1}	R_H^{exp}, Å[a]	N_{ag}	$D_s \times 10^{-10}$, m^2 s^{-1}	R_H^{exp}, Å
CR	0.5[b]	—	—	2.55	10.9	2.2	—	—
	5	—	—	2.51	11.1	2.3	—	—
CPC	—	1.25	—	—	—	—	3.79	7.3
CR + CPC	0.5	2	4/1	2.53[c]	11.0	2.0	0.36	77.4
	1	1	1/1	2.48[c]	11.2	2.1	[d]	—
	5	1.25	1/4	2.51[c]	11.1	2.1	[d]	—
	20	1	1/20	2.38[c]	11.7	2.7	0.68	40.7

[a] Theoretical value of hydrodynamic radii of CR is 8.4 Å. [b] The data from ref. 21c. [c] The diffusion decay of CR signals is single-exponential. [d] The signals of CPC are broadening, and the short values of T2 do not allow determination of the D_s-values.

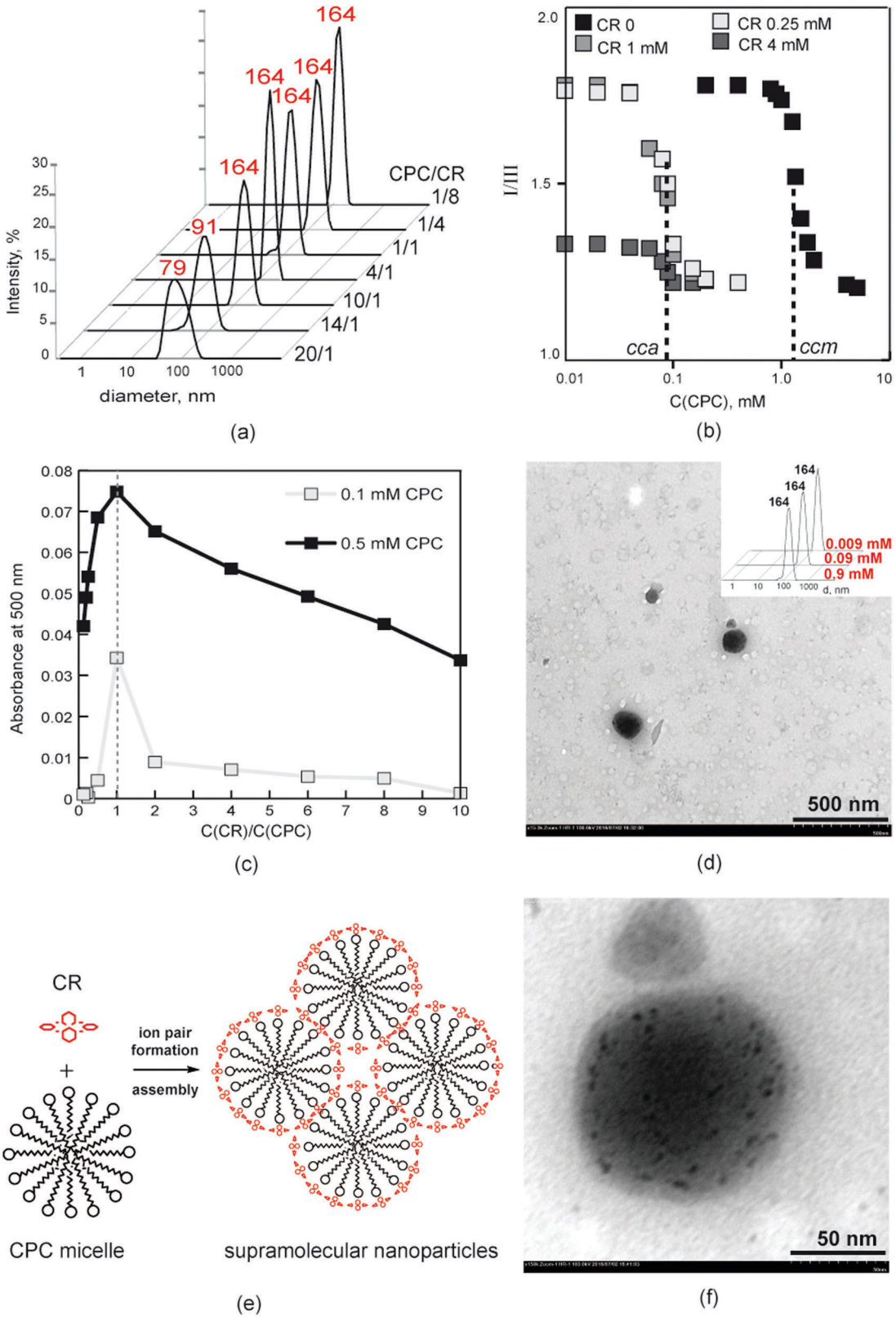

Fig. 2 (a) The intensity-averaged size distribution for CR–CPC solutions with different molar ratios (DLS method, 25 °C; for details see ESI,† Table S2). (b) The dependence of I/III values of pyrene (0.002 mM) on the concentration of CPC in the presence of CR (0, 0.25, 1 and 4 mM). (c) The dependence of the optical density of CR–CPC solutions at 500 nm on the CR/CPC molar ratio in the 0.1 and 0.5 mM CPC solutions. (d and f) TEM of SNPs (CR/CPC 1/1, 0.0909 mM), scale: (d) 500 nm, (f) 50 nm. (d) Inset – the intensity-averaged size distribution for a series of CR–CPC 1/1 dilute solutions. (e) The schematic of CPC–CR association and formation of SNPs.

ratios from 30/1 to 1/10 were opalescent, and solutions with CPC/CR ratios of 1/15 and 1/20 were transparent. In the CPC/CR solution with a molar ratio of 8/1, the compensation of charge is assumed. Thus, precipitation was observed due to the formation of a hydrophobic complex (Fig. S2, ESI†).

The existence of nanosized particles in opalescent solution, the hydrodynamic diameters of which increase as the CPC concentration decreases from 79 nm at a 30-fold excess of CPC to 164 nm at CPC/CR = 10/1, 4/1, 2/1, 1/1, 1/4, 1/8, and 1/10 (Fig. 2a and Table S2, ESI†), was shown by the DLS method. The sizes of the particles in individual solutions of CR (1 mM) and CPC (1 mM) were not estimated by the DLS method because they were too small. The same situation was observed for solutions with 15- and 20-fold excesses of CR. According to ref. 34, the hydrodynamic diameter of a CPC micelle is about 2 nm. Thus, the formation of large associates in the CPC–CR solutions is observed; moreover, in the range of CPC/CR molar ratios from 10/1 to 1/10 (except for 8/1), the particles with close sizes independently on component ratio are formed (Fig. 2a). Probably, under these conditions, similar particles with the same properties are formed. This assumption is confirmed by the zeta potentials of the CPC–CR solutions. For example, the value of the zeta potential of the CPC solution is positive (+82 mV) and the values of CPC/CR 4/1, 1/1, and 1/4 solutions are negative and close to each other (about −60 mV, Table 2). That is, the outer layer of CPC–CR particles consists of macrocyclic anions and the charge of the particle is practically independent of the amount of added macrocycle.

Also, the critical association concentrations (cac) of CPC in the presence of CR were estimated. These were obtained by a fluorimetry method with pyrene as fluorescent probe in solutions with varied CPC concentrations and in the presence of 0, 0.25, 1, and 4 mM CR (Fig. 2b). It should be noted that in the solution, which contains 4 mM of CR, the I/III value of pyrene noticeably decreases (from 1.78 to 1.33 at minimum CPC concentrations, Fig. 2b); this is obviously due to the binding of pyrene near to aromatic rings of macrocycles, which were in excess. As it proved regardless of the amount of macrocycles, the cac of CPC decreased by one order of magnitude (Table 3). Thus, the macrocycle increases its hydrophobicity as it interacts with CPC, which promotes the formation of its associates at lower concentrations of CPC. The lack of influence of the amount of CR on the cac indicates that the same stoichiometry of CPC–CR association occurs in solutions with different macrocycle contents.

Since the supramolecular interaction of CPC–CR leads to opalescence in solutions, the solution having the components in a molar ratio closer to the stoichiometry of the CPC·CR associate should have the maximum optical density. Therefore, the stoichiometry of association was found by studying the absorption of CPC–CR solutions with different molar ratios of the components. Two series of solutions with constant concentrations of CPC (0.1 and 0.5 mM) and varied concentrations of macrocycles (because the aggregation characteristics of CR remain constant over a large range of concentrations[21c]) have been prepared. A plot of the absorbance of the CR–CPC solutions at 500 nm *vs.* the CR/CPC molar ratio shows that a maximum absorbance is observed for a CR/CPC molar ratio of 1/1 in both series (Fig. 2c). This means that the major role in the formation of supramolecular nanoparticles is played by the CPC/CR 1/1 associate.

To identify the character of the interaction in the CPC/CR 1/1 associate, the FT-PGSE NMR method was used, which provides information about the formation of the complex by comparison of the self-diffusion coefficients of the solution components. The solutions with CPC/CR molar ratios of 1/4, 1/1, and 4/1 were studied. Both ^{1}H NMR and FT-PGSE NMR spectra of the mixed solution contained broad signals for CPC, which made it difficult to determine its self-diffusion coefficients (Fig. S3, ESI†). In the solution with excess of the surfactant (CR/CPC 1/4), the signals of CPC became narrower because of its decreasing association (D_s CPC 0.36×10^{10} m^2 s^{-1}). Herewith, neither a lack nor an excess of CPC influence the D_s of CR, and a single-exponential diffusion decay of the CR signals is observed (Table 1).

It was previously shown that inclusion of the macrocyclic molecules into the surfactant micelles led to a decrease in the D_s of the macrocycle approximating to the D_s of the surfactant.[18b,29] In some cases, a two-component diffusion decay can be observed as a result of slow exchange between free and associated macrocyclic molecules.[13a] On the other hand, according to ref. 17d, the formation of a macrocycle–surfactant ion pair results in broadening of the surfactant molecule signals in the spectra, and the D_s of the macrocycle is not decreased. Therefore, we can assume that the formation of an ion pair is observed in CPC–CR solutions.

In the ^{1}H NMR spectra of a solution with a four-fold excess of the macrocycle (CPC/CR 1/4), high-field shifts of the proton signals of pyridinium and the $N^+CH_2CH_2$ groups of CPC are observed (ESI,† Table S3), which may indicate that the head groups of the surfactant molecules are located close to the aromatic fragments of the macrocycle. Also, in the 2D NOESY spectrum of the solution, small cross-peaks are observed between the signals of the protons of the pyridinium group of CPC and those of the $-C_6H_4-O-CH_3$ protons of the macrocycle (Fig. 3).

Table 3 The cac values of CPC in solutions with different concentrations of CR

C(CR), mM	cac, mM
0	1.367
0.25	0.100
1	0.092
4	0.093

Table 2 The values of ξ-potentials and pH of individual solutions of CPC and mixed CPC–CR aqueous solutions

	C, mM			
	CPC	CR	ξ, mV	pH
CPC	1	—	+82	7.12
CPC/CR 4/1	0.98	0.24	−61	7.55
CPC/CR 1/1	0.91	0.91	−58	8.04
CPC/CR 1/4	0.71	2.8	−58	9.86

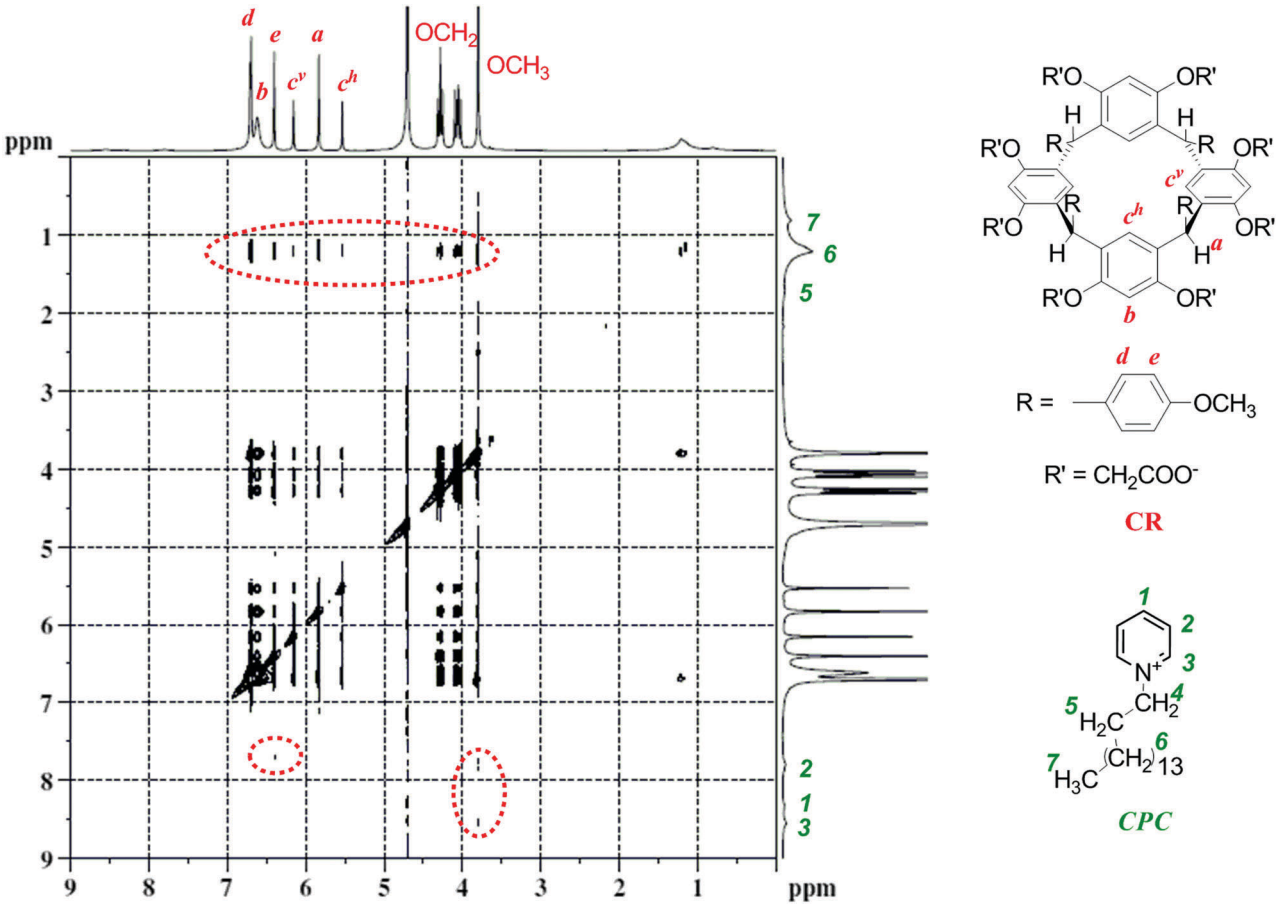

Fig. 3 2D NOESY spectra of CPC/CR (1/4, *C*(CR) = 5 mM) solution in D_2O; the dotted circle indicates the cross peaks between the signals of some groups of CR and CPC.

This probably indicates the existence of a small amount of host–guest complex, the formation of which, however, does not practically influence the D_s of CR; at the same time, the surfactant D_s increases, which is probably due to the involvement of parts of the CPC monomers in closer interactions with the macrocycle (Table 1). In the 2D NOESY spectra of all three solutions (CPC/CR = 1/4, 1/1, and 4/1), cross-peaks are observed between the signals of the protons of the CPC alkyl tail and the protons of practically all the groups of the macrocycle, which may indicate the inclusion of some CR molecules into the CPC associate (Fig. 3). Nevertheless, the formation of the CPC–CR ion pair contributes significantly to the interaction (because of the lack of change in the D_s of the macrocycle). Apparently, the increase in the hydrophobicity of the CPC–CR ion pair compared with that of CPC leads to a decrease in the cac of the surfactant and to the formation of large supramolecular nanoparticles (SNPs).

The morphology of the CPC–CR (1/1) associates was studied by TEM. It was shown that the SNPs are spherical particles with diameters of 70 to 155 nm and consist of smaller particles with diameters of about 2–4 nm (Fig. 2d and f). According to ref. 34, the hydrodynamic diameter of the CPC micelle is 2 nm, so the SNPs consist of CPC micelles united in a cooperative associate. Earlier, it was shown that self-association of CPC in the presence of organic (above 5 mM) and inorganic anions (above 50 mM) leads to the formation of rod-like structures.[27] To the best of our knowledge, the association of CPC micelles into spherical particles has not been previously mentioned.

To confirm the morphology of the SNPs (and the absence of a micelle–rod-like micelle transition) we attempted to investigate the anisotropy of CPC associates in the presence of CR using a fluorescent probe, 1,6-diphenyl-1,3,5-hexatriene (DPH). Unfortunately, binding of DPH by the macrocycle occurred in the CPC–CR solution, and additional facts about the morphology of its co-associates could not be obtained by this method (for details see ESI† and Fig. S4).

Nevertheless, no micelle–rod-like micelle transition for CPC is observed even in the presence of excess macrocycles. Thus, the viscosity of CPC/CR 1/15 and 1/20 solutions is not increased (data are not shown) and the CPC D_s in the CPC/CR 1/20 solution is slightly higher than in the CPC/CR 4/1 solution, while the D_s of CR slightly decreased (Table 1). Thus, the self-association of CPC is decreased in the presence of a 20-fold excess of CR. We assume that this is due to the increase in the amount of the CPC–CR host–guest complex in solution.

Obviously, CR has the potential to be involved in multiple intermolecular interactions due to its molecular structure. Eight anionic groups provide the electrostatic interactions and the aromatic rings are able to form π–π stacking interactions with

the pyridinium group of CPC. To determine how the CR molecule promotes the association of CPC micelles, an analysis of the CR interactions with an analog of CPC, pentylpyridinium bromide (C5Pyr), has been carried out. A Job's plot for the CR–C_5Pyr system has been constructed using ^{1}H NMR (ESI,† Fig. S5). The maximum of the Job's plot is observed at the molar ratio CR/C_5Pyr = 1/2. Herewith, even in the presence of a four-fold excess of CR, chemical shifts of signals of C_5Pyr are small (ESI,† Table S3) and the fraction of bound C_5Pyr is only 34% (ESI,† Table S4). These data are in good agreement with the fact that the existence of CR in the chair conformation leads to the absence of a macrocyclic cavity as such but allows the association of CR with two guest molecules. Probably, the organization of CPC micelles into large associates occurs due to the ability of CR to take part in ditopic binding; as a result, macrocyclic molecules act as ''glue'', as shown in Fig. 2e.

So, in the range of CPC/CR molar ratios from 10/1 to 1/10, the macrocycle forms an ion pair with CPC and induces the association of CPC micelles but this does not lead to a change of their morphology into rod-like micelles.

Based on the obtained data, we assume that the formation of a CR–CPC ion pair leads to an increase in the hydrophobicity of the system and to the assembly of CPC micelles into spherical supramolecular nanoparticles. The ability of the macrocycle to take part in multiple intermolecular interactions allows it to act as ''glue'' for CPC micelles, which results in their unusual association (Fig. 2e).

The stability of SNPs and the investigation of substrate binding

Monitoring of the particle size distribution in CPC–CR solutions with different molar ratios by the DLS method showed that nanoassociates are stable for a month (ESI,† Table S2). SNPs (CPC/CR 1/1) retain their sizes (about 164 nm) when heated to 50 °C (Fig. 4a and ESI,† Table S5) and when diluted to a concentration below the cac (Fig. 2d, inset and ESI,† Table S6). In the presence of electrolytes (0.15 M NaCl or phosphate buffer), hydrophobic interactions in the SNPs become stronger and lead to a solubility limit of 0.1 mM (for details see ESI† and Fig. S6). At low pH values, carboxy groups of CR are protonated and the macrocycle loses its ability to dissolve in water. Thus, SNPs must be pH-sensitive, since the protonation of CR should lead to an increase in their hydrophobicity and to enlargement of the nanoassociates. A study of the sizes of SNPs (CPC/CR 1/1, 0.078 mM, DLS method) in solutions with different pH values (phosphate buffer) showed an increase in the average hydrodynamic particle diameter when the pH was decreased from 8 to 3 (Fig. 4b) and precipitation at pH 2–3 (ESI,† Table S7).

Earlier, it was shown that the formation of macrocycle–surfactant co-associates leads to a decrease in the ability of the surfactant micelles to solubilize.[15,18,19,33] The comparison of UV Vis spectra of water-insoluble dye methyl yellow (MY) solubilized by CPC and SNP (CPC/CR 4/1 and 1/4) solutions showed an almost three-fold decrease in the absorbance intensity of the dye in the SNP solutions (Fig. 5a). CR alone does not solubilize MY. Thus, the presence of CR leads to a decrease in the permeability of the CPC micelles to the water-insoluble MY.

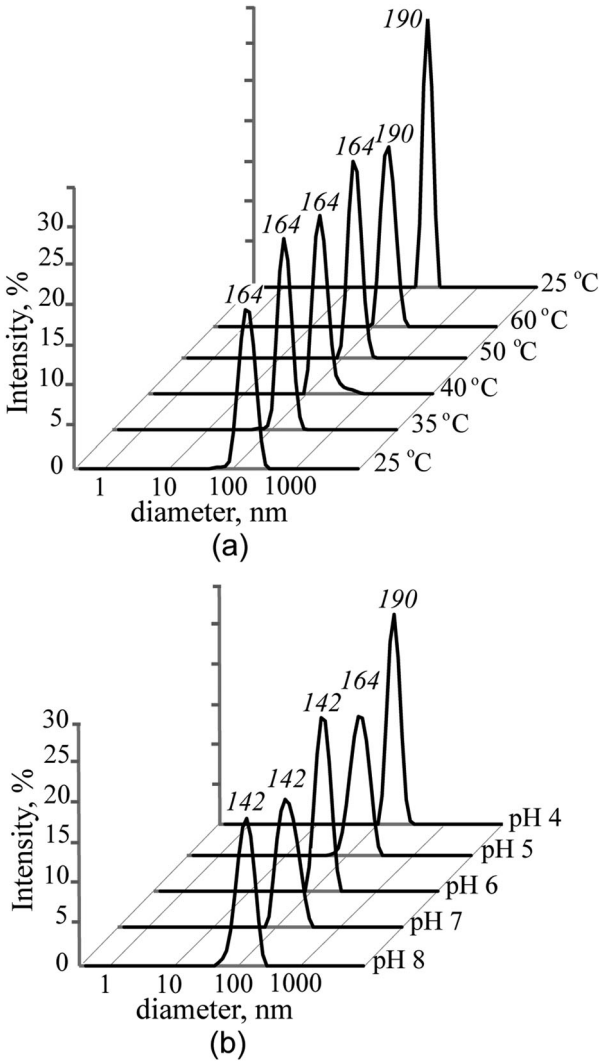

Fig. 4 The intensity-averaged size distribution for SNPs at different temperatures (a, CR/CPC 1/1, 1 mM) and pH values (b, CR/CPC 1/1, 0.078 mM, phosphate buffer).

To investigate the binding properties of the macrocycles in the presence of CPC micelles, the water-soluble fluorescent cationic dye rhodamine 6G (R6G) was used. As a rule, the interaction of fluorescent dyes and macrocycles with a host–guest complex is accompanied by a shift in the maximum of the absorbance band (λ_{max}) and by a change in the emission intensity in the fluorescent spectra of a dye.[35] The absorption and emission spectra of R6G are almost unchanged in the presence of CPC. In the presence of CR (1 mM) and SNPs (CPC/CR 1/1, 1 mM), the λ_{max} of R6G (526 nm) in the absorbance spectra shifts to 529 and 534 nm, respectively (Fig. 5b). In the emission spectra, a decrease in the fluorescence intensity of R6G in the presence of CR is observed, and this increases in the SNP solutions (Fig. 5c). Earlier, it was shown that binding of rhodamine dyes by calixarenes leads to the quenching of their emission.[36] Thus, the change in the spectral properties of R6G indicates the binding of the dye in the presence of CR and CR–CPC associates. The fluorescence titration of R6G by a molar ratio method allowed

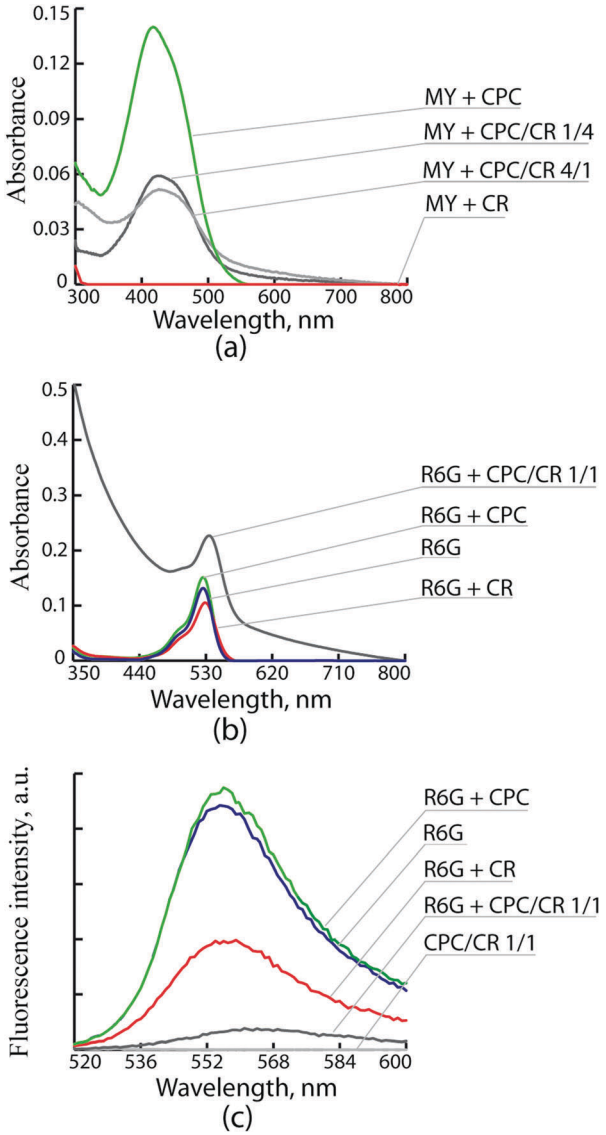

Fig. 5 (a) UV Vis spectra of MY in CR, CPC, and CPC/CR 4/1 and 1/4 solutions. UV Vis spectra (b) and fluorescence spectra (c) of R6G in individual, CR, CPC, and CPC/CR 1/1 solutions (the spectrum of CPC/CR 1/1 solution is added as a blank).

us to obtain the binding constants, which are about 15 000 and 22 000 M^{-1} in the presence of CR and SNPs, respectively (for details see ESI† and Fig. S7). The increase in R6G binding in SNP solutions can be explained by the inclusion of the dye molecules between neighboring molecules of CR, being a layer of counter ions of CPC micelles. Here, the dye molecules are "clamped" between the neighboring macrocyclic molecules, which leads to an increase in dye binding and to the quenching of its emission (ESI,† Fig. S8).

Conclusions

In conclusion, the formation of an ion pair by the anionic macrocyclic CR and cationic surfactant CPC in an aqueous solution, which induces the micellization of CPC at lower concentrations, is demonstrated. Furthermore, these spontaneously associate into SNPs with an average hydrodynamic diameter of 164 nm. The sizes of the SNPs at various CPC/CR concentrations (from 10/1 to 1/10, except for 8/1) are retained from 25–50 °C and pH 8–4. The SNPs are able to solubilize the water-insoluble dye MY in CPC micelles and bind the water-soluble dye R6G *via* the macrocyclic molecules that are located around the nanoparticle surfaces. The co-association of CPC and CR into SNPs leads to a decrease in the permeability of CPC micelles towards a water-insoluble substrate and to an increase in the water-soluble substrate binding. The obtained supramolecular system can be used as a nanocapsule for water-insoluble and water-soluble substrates.

Acknowledgements

Microscopic investigations were carried out in the "transmission electron microscopy" laboratory of Kazan National Research Technological University. The authors gratefully thank Prof. Nefed'ev E.S.

References

1 (*a*) A. A. Karim, Q. Dou, Z. Li and X. J. Loh, *Chem. – Asian J.*, 2016, **11**, 1300–1321; (*b*) Y. Zhou, H. Li and Y.-W. Yang, *Chin. Chem. Lett.*, 2015, **26**, 825–828; (*c*) L. Ya. Zakharova, R. R. Kashapov, T. N. Pashirova, A. B. Mirgorodskaya and O. G. Sinyashin, *Mendeleev Commun.*, 2016, **26**, 457–468; (*d*) G. Yu, K. Jie and F. Huang, *Chem. Rev.*, 2015, **115**, 7240–7303.

2 Y.-X. Wang, D.-Sh. Guo, Y.-Ch. Duan, Y.-J. Wang and Y. Liu, *Sci. Rep.*, 2015, **5**, 9019.

3 (*a*) A. Feng and J. Yuan, *Macromol. Rapid Commun.*, 2014, **35**, 767–779; (*b*) P. J. Honey, J. Rijo, A. Anju and K. P. Anoop, *Acta Pharm. Sin. B*, 2014, **4**, 120–127.

4 (*a*) Zh. Qi and Ch. A. Schalley, *Acc. Chem. Res.*, 2014, **47**, 2222–2233; (*b*) X. Ma and Y. Zhao, *Chem. Rev.*, 2015, **115**, 7794–7839.

5 Pr. Kaur, T. Garg, G. Rath, R. S. R. Murthy and A. K. Goyal, *Drug Delivery*, 2016, **23**, 727–738.

6 S. Lankalapalli and V. R. M. Kolapalli, *Indian J. Pharm. Sci.*, 2009, **71**, 481–487.

7 (*a*) S. dos Santos, B. Medronho, T. dos Santos and F. E. Antunes, in *Drug Delivery Systems: Advanced Technologies Potentially Applicable in Personalised Treatment*, ed. J. Coelho, Springer, 2013, pp. 35–85; (*b*) L. X. Jiang, J. B. Huang, A. Bahramian, P. X. Li, R. K. Thomas and J. Penfold, *Langmuir*, 2012, **28**, 327–338.

8 A. Barbetta, C. La Mesa, L. Muzi, C. Pucci, G. Risuleo and F. Tardani, in *Nanobiotechnology*, ed. W. Ahmed and D. A. Phoenix, One Central Press, 2014, vol. 7, pp. 152–179.

9 (*a*) Sh. Peng, K. Wang, D.-Sh. Guoa and Y. Liu, *Soft Matter*, 2015, **11**, 290–296; (*b*) Ju. E. Morozova, V. V. Syakaev, A. M. Ermakova, Ya. V. Shalaeva, E. Kh. Kazakova and A. I. Konovalov, *Colloids Surf., A*, 2015, **481**, 400–406;

(*c*) E. V. Ukhatskaya, S. V. Kurkov, S. E. Matthews and Th. Loftsson, *J. Inclusion Phenom. Macrocyclic Chem.*, 2014, **79**, 47–55.

10 (*a*) S. A. Ahmed, A. Chatterjee, B. Maity and D. Seth, *J. Photochem. Photobiol., B*, 2016, **161**, 59–70; (*b*) J. H. Mondal, T. Ghosh, S. Ahmed and D. Das, *Langmuir*, 2014, **30**, 11528–11534; (*c*) M. Tsianou and A. I. Fajalia, *Langmuir*, 2014, **30**, 13754–13764; (*d*) A. J. M. Valente and O. Söderman, *Adv. Colloid Interface Sci.*, 2014, **205**, 56–176; (*e*) J. G. Harangozo, V. Wintgens, Z. Miskolczy, J.-M. Guigner, C. Amiel and L. Biczók, *Langmuir*, 2016, **32**, 10651–10658.

11 (*a*) X. Ma and Ya. Zhao, *Chem. Rev.*, 2015, **115**, 7794–7839; (*b*) Sh. Peng, J. Gao, Y. Liu and D.-Sh. Guo, *Chem. Commun.*, 2015, **51**, 16557–16560; (*c*) W.-Ch. Geng, Y.-C. Liu, Y.-Y. Wang, Zh. Xu, Zh. Zheng, Ch.-B. Yang and D.-Sh. Guo, *Chem. Commun.*, 2017, **53**, 392–395; Zh. Xu, Sh. Peng, Y.-Y. Wang, J.-K. Zhang, A. I. Lazar and D.-Sh. Guo, *Adv. Mater.*, 2016, **28**, 7666–7671.

12 R. V. Rodik, V. I. Boyko and V. I. Kalchenko, *Curr. Med. Chem.*, 2009, **16**, 1630–1655.

13 (*a*) Y. Cao, Y. Wang, D. Guo and Y. Liu, *Sci. China: Chem.*, 2014, **57**, 371–378; (*b*) G. Gattuso, A. Notti, A. Pappalardo, S. Pappalardo, M. F. Parisi and F. Puntoriero, *Tetrahedron Lett.*, 2013, **54**, 188–191.

14 N. Basilio, M. Martín-Pastor and L. García-Río, *Langmuir*, 2012, **28**, 6561–6568.

15 T. N. Pashirova, A. Yu. Ziganshina, E. D. Sultanova, S. S. Lukashenko, Yu. R. Kudryashova, E. P. Zhiltsova, L. Ya. Zakharova and A. I. Konovalov, *Colloids Surf., A*, 2014, **448**, 67–72.

16 (*a*) N. Basilio and L. Garcia-Rio, *Chem. – Eur. J.*, 2009, **15**, 9315–9319; (*b*) N. Basilio, M. Martín-Pastor and L. García-Río, *Langmuir*, 2012, **28**, 6561–6568.

17 (*a*) Zh. Li, Ch. Hu, Y. Cheng, H. Xu, Xu. Cao, X. Song, H. Zhang and Y. Liu, *Sci. China: Chem.*, 2012, **55**, 2063–2068; (*b*) K. Wang, D.-S. Guo, X. Wang and Y. Liu, *ACS Nano*, 2011, **5**, 2880–2894; (*c*) V. Francisco, N. Basilio, L. Garcia-Rio, J. R. Leis, E. F. Maques and C. Vázquez-Vázquez, *Chem. Commun.*, 2010, **46**, 6551–6553; (*d*) C. Bize, J.-Ch. Garrigues, M. Blanzat, I. Rico-Lattes, O. Bistri, B. Colasson and O. Reinaud, *Chem. Commun.*, 2010, **46**, 586–588.

18 (*a*) G. A. Gaynanova, A. M. Bekmukhametova, R. R. Kashapov, A. Yu. Ziganshina and L. Ya. Zakharova, *Chem. Phys. Lett.*, 2016, **652**, 190–194; (*b*) R. R. Kashapov, T. N. Pashirova, S. V. Kharlamov, A. Yu. Ziganshina, E. P. Ziltsova, S. S. Lukashenko, L. Ya. Zakharova, W. D. Habicher, Sh. K. Latypov and A. I. Konovalov, *Phys. Chem. Chem. Phys.*, 2011, **13**, 15891–15898.

19 R. R. Kashapov, R. I. Rassadkina, A. Yu. Ziganshina, R. K. Mukhitova, V. A. Mamedov, N. A. Zhukova, M. K. Kadirov, I. R. Nizameev, L. Ya. Zakharova and O. G. Sinyashin, *RSC Adv.*, 2016, **6**, 38548–38552.

20 (*a*) M. Karimi, P. S. Zangabad, A. Ghasemi, M. Amiri, M. Bahrami, H. Malekzad, H. Gh. Asl, Z. Mahdieh, M. Bozorgomid, A. Ghasemi, M. R. R. T. Boyuk and M. R. Hamblin, *ACS Appl. Mater. Interfaces*, 2016, **8**, 21107–21133; (*b*) M. E. Caldorera-Moore, W. B. Liechty and N. A. Peppas, *Acc. Chem. Res.*, 2011, **44**, 1061–1070.

21 (*a*) V. V. Syakaev, E. Kh. Kazakova, Ju. E. Morozova, Ya. V. Shalaeva, Sh. K. Latypov and A. I. Konovalov, *J. Colloid Interface Sci.*, 2012, **370**, 19–26; (*b*) E. Kazakova, Ju. Morozova, D. Mironova, V. Syakaev, L. Muslinkina and A. Konovalov, *Supramol. Chem.*, 2013, **25**, 831–841; (*c*) D. Mironova, L. Muslinkina, V. Syakaev, Ju. Morozova, V. Yanilkin, A. Konovalov and E. Kazakova, *J. Colloid Interface Sci.*, 2013, **407**, 148–154; (*d*) Ju. E. Morozova, V. V. Syakaev, E. Kh. Kazakova, Ya. V. Shalaeva, I. R. Nizameev, M. K. Kadirov, A. D. Voloshina, V. V. Zobov and A. I. Konovalov, *Soft Matter*, 2016, **12**, 5590–5599.

22 (*a*) C. Bonaccorso, S. Gentile, F. G. Gulino and D. Sciotto, *Lett. Org. Chem.*, 2009, **6**, 598–603; (*b*) V. V. Syakaev, A. R. Mustafina, Ju. G. Elistratova, Sh. K. Latypov and A. I. Konovalov, *Supramol. Chem.*, 2008, **20**, 453–460.

23 J. Akbari, M. Saeedi, K. Morteza-Semnani, H. Kelidari and M. Lashkari, *Adv. Pharm. Bull.*, 2014, **4**, 385–390.

24 (*a*) L. M. Schaeffer, G. Szewczyk, J. Nesta, M. Vandeven, L. Du-Thumm, M. I. Williams and E. Arvanitidou, *J. Clin. Dent.*, 2011, **22**, 183–186; (*b*) M. I. Williams, *J. Clin. Dent.*, 2011, **22**, 179–182; (*c*) M. M. Masadeh, S. F. Gharaibeh, K. H. Alzoubi, S. I. Al-Azzam and W. M. Obeidat, *J. Clin. Med. Res.*, 2013, **5**, 389–394.

25 J. Karayil, S. Kumar, Y. Talmon, P. A. Hassan, B. V. R. Tata and L. Sreejith, *J. Surfactants Deterg.*, 2016, **19**, 849–860.

26 T. Mukhim, J. Dey, S. Das and K. Ismail, *J. Colloid Interface Sci.*, 2010, **350**, 511–515.

27 L. Abezgauz, K. Kuperkar, P. A. Hassan, O. Ramon, P. Bahadur and D. Danino, *J. Colloid Interface Sci.*, 2010, **342**, 83–92.

28 J. Bhattacharjee, V. K. Aswal, P. A. Hassan, R. Pamu, J. Narayananc and J. Bellare, *Soft Matter*, 2012, **8**, 10130–10140.

29 Sh. D. Choudhury, N. Barooah, V. K. Aswal, H. Pal, A. C. Bhasikuttana and J. Mohanty, *Soft Matter*, 2014, **10**, 3485–3493.

30 J. G. de la Torre, M. L. Huertas and B. Carrasco, *J. Magn. Reson.*, 2000, **147**, 138–146.

31 G. B. Ray, I. Chakraborty and S. P. Moulik, *J. Colloid Interface Sci.*, 2006, **294**, 248–254.

32 (*a*) I. R. Knyazeva, V. I. Sokolova, M. Gruner, W. D. Habicher, V. V. Syakaev, V. V. Khrizanforova, B. M. Gabidullin, A. T. Gubaidullin, Yu. H. Budnikova, A. R. Burilov and M. A. Pudovik, *Tetrahedron Lett.*, 2013, **54**, 3538–3542; (*b*) I. R. Knyazeva, V. I. Matveeva, V. V. Syakaev, B. M. Gabidullin, A. T. Gubaidullin, M. Gruner, W. D. Habicher, A. R. Burilov and M. A. Pudovik, *Tetrahedron Lett.*, 2014, **55**, 7209–7214.

33 S. V. Kharlamov, R. R. Kashapov, T. N. Pashirova, E. P. Zhiltsova, S. S. Lukashenko, A. Yu. Ziganshina, A. T. Gubaidullin, L. Ya. Zakharova, M. Gruner, W. D. Habicher and A. I. Konovalov, *J. Phys. Chem. C*, 2013, **117**, 20280–20288.

34 D. Varade, T. Joshi, V. K. Aswal, P. S. Goyal, P. A. Hassan and P. Bahadur, *Colloids Surf., A*, 2005, **259**, 95–101.

35 R. N. Dsouza, U. Pischel and W. M. Nau, *Chem. Rev.*, 2011, **111**, 7941–7980.

36 Y.-J. Zhang, W.-X. Cao and J. Xu, *Chin. J. Chem.*, 2002, **20**, 322–326.